Lattice QCD matrix elements for the $B_s^0 - \bar{B}_s^0$ width difference beyond leading order

Christine T. H. Davies,[1] Judd Harrison,[2,1] G. Peter Lepage,[3]
Christopher J. Monahan,[4,5,6] Junko Shigemitsu,[7] and Matthew Wingate[2,a]
(HPQCD Collaboration),[b]

[1]*SUPA, School of Physics and Astronomy, University of Glasgow, Glasgow, G12 8QQ, United Kingdom*
[2]*DAMTP, University of Cambridge, Cambridge CB3 0WA, United Kingdom*
[3]*Laboratory of Elementary Particle Physics, Cornell University, Ithaca, NY 14853, United States*
[4]*Institute for Nuclear Theory, University of Washington, Seattle, WA 98195-1550, United States*
[5]*Physics Department, College of William and Mary, Williamsburg, VA 23187, United States*
[6]*Thomas Jefferson National Accelerator Facility, Newport News, VA 23606, United States*
[7]*Department of Physics, Ohio State University, Columbus, OH 43210, United States*

Predicting the $B_s^0 - \bar{B}_s^0$ width difference $\Delta\Gamma_s$ relies on the heavy quark expansion and on hadronic matrix elements of $\Delta B = 2$ operators. We present the first lattice QCD results for matrix elements of the dimension-7 operators $R_{2,3}$ and their linear combinations, $\tilde{R}_{2,3}$, using nonrelativistic QCD for the bottom quark and a highly improved staggered quark (HISQ) action for the strange quark. Computations use MILC ensembles of gauge field configuations with $2+1+1$ flavors of sea quarks with the HISQ discretization, including lattices with physically light up/down quark masss. We discuss features unique to calculating matrix elements of these operators and analyze errors due to series truncation, discretization, and quark mass dependence. Finally we report the first Standard Model determination of $\Delta\Gamma_s$ using lattice QCD results for all hadronic matrix elements through $O(1/m_b)$.

Version compiled 20 September 2019, 14:56.

I. INTRODUCTION

Oscillations of neutral mesons into their antiparticles have been important phenomena in the study of quark flavor. This flavor-changing, neutral mixing is absent in the Standard Model (SM) at the classical level; appearing at one-loop level it is suppressed by two powers of Fermi's constant G_F relative to hadronic and quark mass scales. A few observables are, to a high level of precision, sensitive only to short-distance physics. Within the Standard Model predictions for these are reliably calculable because the dominant contribution comes from top-quark loops; there is no significant contribution from intermediate-state hadronic physics. Prime examples are: in the mixing of strange mesons $K^0 - \bar{K}^0$, the indirect CP-violating ratio ϵ_K and, in beauty mesons $B^0_{d,s} - \bar{B}^0_{d,s}$, the the mass differences (equivalently, the oscillation frequencies) $\Delta M_{d,s}$. Precise experimental measurements of these, together with accurate Standard Model predictions, constitute stringent tests of the SM description of quark flavor.

Beyond these observables are others, where contributions from hadronic intermediate states must be included. For example, mixing in neutral charm mesons $D^0 - \bar{D}^0$ has significant long-distance contributions due to differing flavor structure from K^0 and B^0 mixing. Predictions for heavy meson and baryon lifetimes also require theoretical treatment of long-distance effects.

The $B_s^0 - \bar{B}_s^0$ width difference $\Delta\Gamma_s$ is another example and is the focus of this paper. Unlike the mass difference, which comes from the real part of the mixing amplitude, the width difference comes from the imaginary part of the amplitude which, by the optical theorem, describes the decays to real final states, primarily $b \to c\bar{c}s$ decays. Since we expect $\Delta\Gamma_s$ to be insensitive to new physics, comparison between theory and experiment is a test of the theoretical methods involved. Agreement here is a necessary condition for trusting these methods to reliably yield a SM prediction for quantities where new physics could contribute more prominently, e.g. in $D^0 - \bar{D}^0$ mixing.

Predicting the SM width difference $\Delta\Gamma_s$ requires the determination of matrix elements of a nonlocal product of effective operators $H_{\rm eff}^{\Delta F=1}$, with charm and up quarks in the virtual loops. Direct calculation of $\langle B_s^0 | \mathcal{T}\{H_{\rm eff}^{\Delta F=1}(x) H_{\rm eff}^{\Delta F=1}(0)\} | \bar{B}_s^0 \rangle$ using lattice QCD is not presently feasible. Therefore, an additional theoretical approximation is necessary in order to obtain a Standard Model prediction for $\Delta\Gamma_s$, namely the heavy quark expansion (HQE). This expansion makes use of the large b-quark mass compared to the c-quark and other scales in the problem such as $\Lambda_{\rm QCD}$, and approximates the imaginary part of the matrix elements above by a power series in $1/m_b$, composed of matrix elements of local, $\Delta F = 2$ operators such as those appearing in $H_{\rm eff}^{\Delta F=2}$ [1]. (See Ref. [2] for a recent review of the HQE applied to $\Delta\Gamma_s$.)

Matrix elements of the leading, dimension-6 operators in $H_{\rm eff}^{\Delta F=2}$ have been calculated using lattice QCD with increasing precision, motivated by their impact on predictions for $\Delta M_{d,s}$. Results are now available from several groups [3–6] (see Ref. [7] for a review). The precision of these determinations has become good enough that matrix elements of higher-dimension operators are needed

[a] M.Wingate@damtp.cam.ac.uk
[b] http://www.physics.gla.ac.uk/HPQCD

in order to reduce the SM uncertainty in $\Delta\Gamma_s$. Current estimates for the higher-dimension matrix elements come from the vacuum saturation approximation. The lack of any full QCD calculation of dimension-7 operators is a leading uncertainty in the Standard Model determination of $\Delta\Gamma_s$ [2, 8].

In this paper, we provide results of the first complete lattice QCD calculation needed for $\Delta\Gamma_s$ through $O(1/m_b)$. The goal here is to replace order-of-magnitude estimates based on the vacuum saturation approximation with first principles calculations including a quantitative analysis of errors. In this first step, we neglect $\mathcal{O}(\alpha_s)$ corrections to the dimension-7 operators. Including these corrections would involve a technically challenging perturbative calculation going beyond what has been done for the dimension-6 operators [9, 10]. This improvement is left as a future project.

We begin by setting some notation. The convention used for the dimension-6 operators is

$$\begin{aligned} Q_1 &= (\bar{b}^\alpha\gamma^\mu(1-\gamma^5)s^\alpha)(\bar{b}^\beta\gamma_\mu(1-\gamma^5)s^\beta)\,, \\ Q_2 &= (\bar{b}^\alpha(1-\gamma^5)s^\alpha)(\bar{b}^\beta(1-\gamma^5)s^\beta)\,, \\ Q_3 &= (\bar{b}^\alpha(1-\gamma^5)s^\beta)(\bar{b}^\beta(1-\gamma^5)s^\alpha)\,. \\ Q_4 &= (\bar{b}^\alpha(1-\gamma^5)s^\alpha)(\bar{b}^\beta(1+\gamma^5)s^\beta) \\ Q_5 &= (\bar{b}^\alpha(1-\gamma^5)s^\beta)(\bar{b}^\beta(1+\gamma^5)s^\alpha)\,. \end{aligned} \tag{1}$$

At higher order in the HQE, one needs matrix elements of the following operators

$$\begin{aligned} R_0 &= Q_2 + \alpha_1 Q_3 + \frac{1}{2}\alpha_2 Q_1 \\ R_1 &= \frac{m_s}{m_b}(\bar{b}^\alpha(1-\gamma^5)s^\alpha)(\bar{b}^\beta(1+\gamma^5)s^\beta) = \frac{m_s}{m_b}Q_4 \\ R_2 &= \frac{1}{m_b^2}(\bar{b}^\alpha\overleftarrow{D}_\rho\gamma^\mu(1-\gamma^5)D^\rho s^\alpha)(\bar{b}^\beta\gamma_\mu(1-\gamma^5)s^\beta) \\ R_3 &= \frac{1}{m_b^2}(\bar{b}^\alpha\overleftarrow{D}_\rho(1-\gamma^5)D^\rho s^\alpha)(\bar{b}^\beta(1-\gamma^5)s^\beta) \end{aligned} \tag{2}$$

as well as the color-rearranged partners $\tilde{R}_1$, $\tilde{R}_2$, and $\tilde{R}_3$. The perturbative coefficients α_1 and α_2 are given in Refs. [11–13]. Matrix elements of R_0, R_1, and $\tilde{R}_1$ can be inferred from matrix elements of Q_{1-5}. Using Fierz identities and neglecting terms at higher order in $1/m_b$ we have

$$\begin{aligned} \tilde{R}_2 &= -R_2 \\ \tilde{R}_3 &= R_3 + \frac{R_2}{2}\,. \end{aligned} \tag{3}$$

In our formulation, nonrelativistic lattice QCD, these relations (3) hold exactly. Our task will be to compute matrix elements of R_2 and R_3.

II. DESCRIPTION OF LATTICE CALCULATION

We carry out our calculations using gauge field configurations generated by the MILC Collaboration [14–16]. These include the effects of $2+1+1$ flavors of sea quarks using the HISQ fermion action [17, 18]. We use five separate ensembles (see Table I). Two of the ensembles have all of the quark masses tuned to be close to their physical values; these have lattice spacing of 0.12 and 0.15 fm. The other three ensembles span 3 lattice spacings from 0.09 to 0.15 fm, with unphysically large light-quark masses corresponding to pion masses of about 300 MeV. Our use of three lattice spacings allows us to estimate discretization errors, and the computations done with unphysical light quark masses gives us information with which to correct any slight quark mass mistunings.

The lattice actions used are the same as in our recent study of the dimension-6 operator matrix elements [6]. Correlation functions are computed using the HISQ action for the strange quark; the valence quark mass is tuned to be closer to the physical strange mass than the value which was used for the sea strange quark. The nonrelativistic QCD (NRQCD) action [19] is used for the bottom quark. Table II lists the input values used for the relevant parameters. Because the determination of $\langle R_2\rangle$ and $\langle R_3\rangle$ here will have an $O(\alpha_s)$ uncertainty due to tree-level matching between lattice and continuum regularization schemes, we only need a fraction of the statistics used in Ref. [6]. We will occasionally refer to Ref. [6] as the high-statistics companion to this work. Throughout this paper we will use the abbreviated notation $\langle\cdot\rangle \equiv \langle B_s|\cdot|\bar{B}_s\rangle$.

Let us examine a unique feature of computing $\langle R_2\rangle$ and $\langle R_3\rangle$. In the rest frame of the heavy quark, only the temporal component of the following bilinear is important at $1/m_b$ order

$$\frac{1}{m_b^2}(\bar{b}^\alpha\overleftarrow{D}_\rho\Gamma D^\rho s^\alpha) = \pm\frac{1}{m_b}(\bar{b}^\alpha\Gamma D^0 s^\alpha) + \mathcal{O}\left(\frac{1}{m_b^2}\right) \tag{4}$$

where the sign is determined by whether the temporal derivative acts on an outgoing heavy quark or an incoming heavy antiquark. Γ represents either $\gamma^\mu(1-\gamma^5)$ (R_2) or $1-\gamma^5$ (R_3). Using the equation of motion for the strange quark, and neglecting contributions of $\mathcal{O}(m_s/m_b)$,

$$\hat{R}_{2,3} = \pm\frac{1}{m_b}(\bar{b}^\alpha\Gamma\gamma_0\boldsymbol{\gamma}\cdot\mathbf{D}s^\alpha)(\bar{b}^\beta\Gamma s^\beta) \tag{5}$$

and similarly for $\hat{\tilde{R}}_{2,3}$. From this we that, in order to implement the derivative operator, the calculation of the associated three-point correlation functions will require new strange quark propagators with point-split inversion sources at the operator location. We use a symmetric difference operator in each of the spatial dimensions as the source for the inversion of the HISQ Dirac matrix on Coulomb-gauge-fixed configurations. Note we use a hat on an operator when we wish to call attention to the 4-quark operator computed directly on the lattice, in distinction to a linear combination such as a renormalized, matched, or subtracted operator.

TABLE I: Parameters of the MILC $n_f = 2+1+1$ HISQ configurations used. Masses listed are sea quark masses. Lattice spacing determined using the Υ splittings, as in Table I of [20]; errors are statistical, NRQCD systematic, experiment respectively.

Label	a/fm	am_l	am_s	am_c	$N_s^3 \times N_t$	#
VC5	0.1474(5)(14)(2)	0.013	0.0650	0.838	$16^3 \times 48$	1020
VCp	0.1450(3)(14)(2)	0.00235	0.0647	0.831	$32^3 \times 48$	1000
C5	0.1219(2)(9)(2)	0.0102	0.0509	0.635	$24^3 \times 64$	1052
Cp	0.1189(2)(9)(2)	0.00184	0.0507	0.628	$48^3 \times 64$	1000
F5	0.0873(2)(5)(1)	0.0074	0.037	0.440	$32^3 \times 96$	1008

TABLE II: Valence quark parameters, with $c_2 = c_3 = 1$.

Ensemble	$am_s^{\rm val}$	am_b	u_{0L}	$c_1 = c_6$	c_4	c_5
VC5	0.0641	3.297	0.8195	1.36	1.22	1.21
VCp	0.0628	3.25	0.819467	1.36	1.22	1.21
C5	0.0522	2.66	0.834	1.31	1.20	1.16
Cp	0.0507	2.62	0.834083	1.31	1.20	1.16
F5	0.0364	1.91	0.8525	1.21	1.16	1.12

As discussed below, we will also need matrix elements of the dimension-6 operators $\hat{Q}_1$ and $\hat{Q}_2$. At no additional cost, we recompute these here and check that they agree with the high-statistics study [6].

III. FITTING CORRELATION FUNCTIONS

In order to determine the energies and amplitudes associated with the meson creation and annihilation operators, we perform multi-exponential Bayesian fits [21]. The fit functions for the two-point and three-point functions are, respectively,

$$C_{ab}^{\rm 2pt}(t) = \sum_{i=0}^{N_{\rm 2pt}-1} X_{a,i}X_{b,i}e^{-E_i t} - (-1)^{t/a}Y_{a,i}Y_{b,i}e^{-E_i^o t} \tag{6}$$

and, abbreviating terms containing any Y parameters,

$$C_{ab}^{\rm 3pt}(t,T) = \sum_{i,j=0}^{N_{\rm 3pt}-1} X_{a,i}V_{nn,ij}X_{b,j}e^{-E_i t}e^{-E_j(T-t)} + \text{osc.} \tag{7}$$

In practice, we fit to energy differences for all but the ground state energy E_0. The X and Y parameters are the amplitudes for meson creation/annihilation. The labels a and b run over the 3 types of smearings used with the B_s meson interpolating operators, a local operator and two Gaussian-smeared operators with different widths [22]. The $V_{nn,ij}$ are parameters related to the matrix elements of 4-quark operators. Not all fit parameters are well-constrained by the data, so we introduce Bayesian priors as we described in detail in Ref. [23].

We take the two-point functions from earlier studies of $B_{(s)}$ decay constants [20, 22]; these were obtained with 16 time sources on each gauge-field configuration, allowing precise determination of the ground state energies and decay amplitudes. Given that our determinations of the matrix element of $R_{2,3}$ will have $O(\alpha_s)$ truncation errors, we do not need such high statistics. The three-point correlators in this work come from using just 2 times sources on each configuration. One consequence of this difference in statistical accuracy is that a good fit requires more exponentials in (6) than in (7). In fact we observed that if $N_{\rm 3pt}$ is too large, the many poorly determined $V_{nn,jj}$ can spoil the fitter's convergence.

The best approach in this case is to use chained [24], marginalized fits [25]. The high-statistics two-point functions are fit using $N_{\rm 2pt} = 5$. The resulting E_0 and $X_{a,0}$, central values and errors, are used as priors for the fits to the three-point functions. Excited state contamination is accounted for in the three-point functions by incorporating noisy estimates using the results of the two-point fits, then fitting using $N_{\rm 3pt} = 1$. This is akin to cancelling excited-state contamination by dividing three-point functions by appropriate two-point functions.

IV. DISCUSSION OF SUBTRACTION

The prediction of a matrix element of a higher dimension operator using lattice NRQCD is complicated by mixing with lower dimension operators [26]. The presence of the lattice cutoff a means that the matrix elements $\langle \hat{R}_{2,3} \rangle$ will contain contributions from $\langle \hat{Q}_i \rangle$ of the order $O(\alpha_s/(am_b))$. We have used lattice perturbation theory to determine the perturbative coefficients ξ_{ij} which cancel this mixing at one-loop level. Matrix elements of the subtracted operator,

$$R_i^{\rm sub} = \hat{R}_i - \alpha_V \xi_{ij} \hat{Q}_j \,, \tag{8}$$

will have power-law mixing cancelled through $O(\alpha_s)$. For the numerical value of the strong coupling constant, we use $\alpha_V(2/a)$ (Table I of [22], inferred from the work of [27, 28]). The coefficients ξ_{ij} have not been calculated before. The procedure is a straightforward extension of Ref. [10], in particular Sec. IV.B. In this instance the derivative acts on the light quark propagator instead of the heavy quark propagator. Numerical values are tabulated in Table III.

Fig. 1 illustrates the effect of the subtraction (8). The fact that the matrix element of the subtracted operator is 50-70% of the unsubtracted operator shows that this subtraction is significant. This is of comparable size to the mixing seen in the $1/m_b$ contributions to the B and B_s decay constants [26, 29] and matrix elements $\langle Q_j \rangle$ [30]. It is notable that, at least at $O(\alpha_s)$, the size of the subtraction is independent of a over the range of lattice spacings used.

While we perform separate fits to the correlation functions associated with each $\hat{R}_{2,3}$ and $\hat{Q}_i$ in order to study

TABLE III: Coupling constant [22] and perturbative coefficients used in (8), for the values of am_b used on each ensemble.

Coeff	VC5	VCp	C5	Cp	F5
$\alpha_V(2/a)$	0.346	0.343	0.311	0.307	0.267
ξ_{21}	−0.1311	−0.1327	−0.1557	−0.1573	−0.2004
ξ_{22}	0.0092	0.0093	0.013	0.0133	0.0225
ξ_{31}	−0.0331	−0.0334	−0.0392	−0.0397	−0.0508
ξ_{32}	−0.2829	−0.2864	−0.3404	−0.3449	−0.451

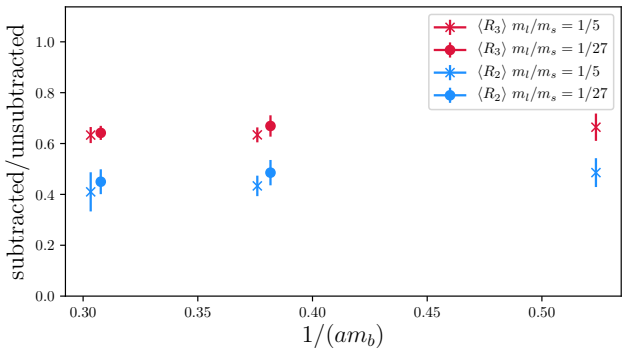

FIG. 1: Ratios of subtracted to unsubtracted matrix elements plotted vs. $1/am_b$. Within the range of parameters used, the size of the subtraction is independent of am_b.

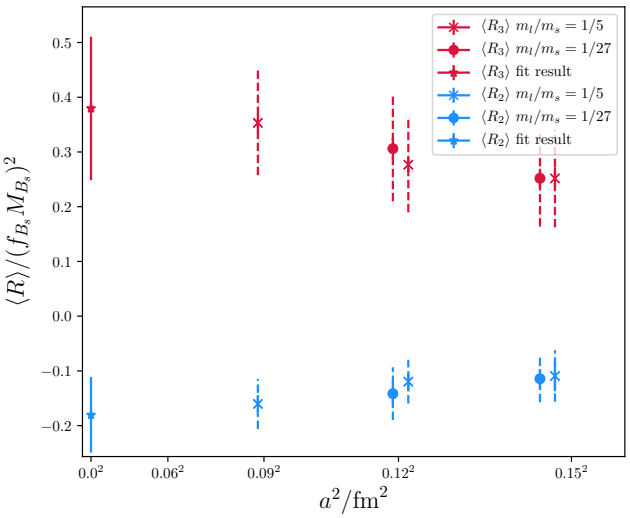

FIG. 2: Matrix elements of R_2 and R_3 plotted against lattice spacing squared. The solid error bars indicate statistical errors only; the dashed errors include the uncertainty due to truncated terms in the weak coupling expansion. The green stars correspond to fit results with $a = 0$ and the physical pion mass.

the relative contributions to the subtracted matrix elements, for the main results we perform fits to linear combinations of three-point functions so that the subtracted matrix element is directly extracted from the fit. This allows correlations to be propagated straightforwardly.

We must estimate the uncertainty due to not knowing the $O(\alpha_s)$ $\overline{\text{MS}}$-to-lattice matching of the R operators nor the $O(\alpha_s^2)$ contributions from the dimension-6 operators. Both of these are suppressed by a power of α_s compared to matrix elements of the two terms in (8). Therefore, we include these truncation errors in our results by multiplying our results by a noisy estimator

$$\langle R_i\rangle = \langle \hat{R}_i - \alpha_V \xi_{ij}\hat{Q}_j\rangle(1+\alpha_V\delta_{am_b}) \tag{9}$$

where $\delta_{am_b} = 0 \pm 1$ is a Gaussian-distributed random variable, one for each of the 3 lattice spacings.

V. CHIRAL-CONTINUUM FIT, SYSTEMATIC ERRORS

Our calculations include numerical data obtained with all quark masses tuned close to their physical values. In order to include some data with unphysically large values for the up/down sea quark masses, we assume an analytic dependence on these masses. We also parametrize discretization errors, e.g. due to the gluon and staggered fermion actions, in powers of $(a\Lambda_{\text{QCD}})^2$. Results presented here come from fits to

$$\frac{\langle R_j\rangle}{f_{B_s}^2 M_{B_s}^2} = \beta\Big[1 + d_2(a\Lambda_{\text{QCD}})^2 + d_4(a\Lambda_{\text{QCD}})^4 + c_1^{s,\text{val}} x_s + c_1^{\text{sea}}(2x'_\ell + x'_s)\Big], \tag{10}$$

where sea quark mass dependence is parametrized by $x'_\ell = M_\pi^2/(2\Lambda_\chi)^2$ and $x'_s = (2M_K^2 - M_\pi^2)/(2\Lambda_\chi)^2$, with $\Lambda_\chi = 1$ GeV. We use the lattice masses aM_π and aM_K tabulated in [16]. For the valence strange quark $x_s = M_{\eta_s}^2/(2\Lambda_\chi)^2$, the η_s being a fictitious flavor-nonsinglet $\bar{s}s$ pseudoscalar meson, which is nevertheless well-defined in chiral perturbation theory. Values for aM_{η_s} on these ensembles [31] are used to parametrize the difference between the input valence strange quark mass and the physical one, using for the "physical" value $M_{\eta_s} = 685.8(4)$ MeV [32]. We assume Gaussian priors of 0 ± 1 for the fit parameters, except for d_2, which we take to be 0 ± 5. In the fits, we find $|d_2| \approx 2.5 \pm 2.0$.

As one would expect, any sensitivity of the $B_s - \bar{B}_s$ matrix elements to the light sea quark mass is much smaller than our uncertainties. The slight mistunings in the sea

TABLE IV: Results for bag factors. The right column uses $M_{B_s} = 5.36688(17)$ GeV [33] and $m_b^{\rm pow} = 4.70(10)$ GeV [12].

Operator k	B'_k	B_k
R_2	0.27(10)	0.89(38)
$\tilde{R}_2$	0.27(10)	0.89(38)
R_3	0.33(11)	1.07(42)
$\tilde{R}_3$	0.35(13)	1.14(46)

or valence strange quark masses are not large enough to give a nonzero result for c_1^s parameters. Including terms quadratic in the x variables has no effect on the fit. Similarly, we obtain d_4 consistent with zero. Within errors the data is completely consistent with a mild a^2 dependence and no quark mass dependence.

Our main results are for the pair of matrix elements

$$\langle B_s|R_2|\bar{B}_s\rangle = -(0.18 \pm 0.07) f_{B_s}^2 M_{B_s}^2 \tag{11}$$

$$\langle B_s|R_3|\bar{B}_s\rangle = (0.38 \pm 0.13) f_{B_s}^2 M_{B_s}^2 \tag{12}$$

or for the linearly dependent color-rearranged operator matrix elements

$$\langle B_s|\tilde{R}_2|\bar{B}_s\rangle = (0.18 \pm 0.07) f_{B_s}^2 M_{B_s}^2 \tag{13}$$

$$\langle B_s|\tilde{R}_3|\bar{B}_s\rangle = (0.29 \pm 0.10) f_{B_s}^2 M_{B_s}^2 \,. \tag{14}$$

At the accuracy with which we work, these results can be interpreted as the $\overline{\rm MS}$-scheme results at the scale $\mu_2 = m_b$, with an uncertainty included to account for the fact that the lattice-continuum matching is tree-level.

It is sometimes convenient to include a numerical factor which arises from the vacuum saturation approximation (VSA). We define B'-factors as follows:

$$B'_{R_2} = -\frac{3}{2}\frac{\langle B_s|R_2|\bar{B}_s\rangle}{f_{B_s}^2 M_{B_s}^2}\,, \quad B'_{\tilde{R}_2} = \frac{3}{2}\frac{\langle B_s|\tilde{R}_2|\bar{B}_s\rangle}{f_{B_s}^2 M_{B_s}^2}$$

$$B'_{R_3} = \frac{6}{7}\frac{\langle B_s|R_3|\bar{B}_s\rangle}{f_{B_s}^2 M_{B_s}^2}\,, \quad B'_{\tilde{R}_3} = \frac{6}{5}\frac{\langle B_s|\tilde{R}_3|\bar{B}_s\rangle}{f_{B_s}^2 M_{B_s}^2}\,. \tag{15}$$

The "unprimed" bag factors B_i which are equal to 1 in the VSA include a mass factor such that [1]

$$B'_i = \left[\frac{M_{B_s}^2}{(m_b^{\rm pow})^2} - 1\right] B_i \,. \tag{16}$$

These B_i are the ones taken in recent phenomenological estimates [2, 8, 12] to be 1.0 ± 0.5 in the absence of a QCD calculation. We tabulate numerical results of our work in Table IV. It turns out that the VSA expectation is a reasonable back-of-the-envelope estimate. (Note that while the bag factors depend on the definition of $m_b^{\rm pow}$, the B'-factors do not.) Our results replace the rough estimates with a lattice QCD computation with all uncertainties quantified.

The matrix elements determined in Ref. [6] allow determination of the remaining 3 matrix elements $B'_{R_0} = -\frac{3}{4}\langle B_s|R_0|\bar{B}_s\rangle/(f_{B_s}M_{B_s})^2 = 0.32(13)$, $B'_{R_1} = \frac{3}{7}\langle B_s|Q_4|\bar{B}_s\rangle/(f_{B_s}M_{B_s})^2 = 1.564(64)$, and $B'_{\tilde{R}_1} = \frac{3}{5}\langle B_s|Q_5|\bar{B}_s\rangle/(f_{B_s}M_{B_s})^2 = 1.167(46)$.

VI. $\Delta\Gamma_s$ IN THE STANDARD MODEL

Our results permit the first lattice determination of $\Delta\Gamma_{1/m_b}$, the power-law corrections to $\Delta\Gamma_s$. Recently there has been an investigation of scale and scheme dependence of the leading term in $\Delta\Gamma_s$, where it has been proposed to include corresponding uncertainties as follows [13]

$$\Delta\Gamma_s = [1.86(17)B_1 + 0.42(3)B'_3] f_{B_s}^2 + \Delta\Gamma_{1/m_b} \tag{17}$$

in the $\overline{\rm MS}$ scheme. Taking $f_{B_s} = 0.2307(12)$ GeV from Ref. [34] and weighted averages of $B_1 = 0.84(3)$ and $B'_3 = 1.36(8)$ from Refs. [5, 6] – the 4% correlation between them is negligible – yields a result for the leading order contribution, $\Delta\Gamma_s^{\rm LO} = 0.114(9)$ ps^{-1}.

The $1/m_b$ contribution to $\Delta\Gamma_s$ can be expressed as a linear combination of the matrix elements of the R operators, times perturbative coefficients γ_k [1, 12]. Writing $\Delta\Gamma_{1/m_b} = -2\tilde{\Gamma}_{12,1/m_b}\cos\phi_{12}$, we have

$$\tilde{\Gamma}_{12,1/m_b} = \frac{G_F^2 f_{B_s}^2 M_{B_s} m_b^2}{24\pi} \sum_k \gamma_k(\bar{z}) B'_{R_k} \,. \tag{18}$$

Here k is an index that runs over the 4 operators in (2) plus the 3 color-rearranged operators. The $\gamma_k(\bar{z})$ are related to the $g_k(\bar{z})$ of [12] by the numerical coefficients relating the matrix elements to the B' factors; additionally γ_1 and $\tilde{\gamma}_1$ include a factor of $\bar{m}_s(\bar{m}_b)/\bar{m}_b(\bar{m}_b) \approx 0.019$. The functions $g_k(\bar{z})$ depend on $\bar{z} = (\bar{m}_c(\bar{m}_b)/\bar{m}_b(\bar{m}_b))^2$ [35] and the leading order $H^{\Delta F=1}$ Wilson coefficients $C_1^{(0)}$ and $C_2^{(0)}$ (numerical values taken from Table 2 of Ref. [13]). For the charm quark mass we use the world average [36] of lattice results with $2+1+1$ flavors of sea quarks [28, 36–38], and for the bottom mass we use the result from Ref. [38]. Numerical values used here are given in Table V. Note that only the terms with B'_{R_0}, B'_{R_2}, and $B'_{\tilde{R}_2}$ contribute to $\Delta\Gamma_{1/m_b}$ due to the smallness of the other γ_k.

Our result is

$$\tilde{\Gamma}_{12,1/m_b} = 0.0110(52) \text{ ps}^{-1} \tag{19}$$

which, given $\cos\phi_{12} = 1$ to the precision relevant here, contributes to the width difference as

$$\Delta\Gamma_{1/m_b} = -2\tilde{\Gamma}_{12,1/m_b} = -0.022(10) \text{ ps}^{-1} \,. \tag{20}$$

The uncertainty in (20) is dominated by that of $\langle\tilde{R}_2\rangle$. From studies of the leading $\Delta\Gamma_s$ term, we expect scale and scheme uncertainties here to similarly be at the 10% level, i.e. not significant compared to the present hadronic uncertainty.

Again using f_{B_s} from [34], the VSA estimate quoted in Ref. [13] is $\Delta\Gamma_{1/m_b} = -0.029(15)$ ps^{-1}. Our result (20) replaces the VSA estimates with unquenched lattice QCD results and reduces the uncertainty on $\Delta\Gamma_{1/m_b}$.

TABLE V: Numerical values used in this Standard Model prediction of $\Delta\Gamma_{1/m_b}$. The quark masses and Wilson coefficients determine the γ coefficients (using $\bar{z}$). Errors in these tabulated values are much smaller than in the matrix elements they multiply.

quantity	value
$\bar{m}_c(\bar{m}_c)$/GeV	1.2753(65)
$\bar{m}_c(\bar{m}_c)/\bar{m}_c(\bar{m}_b)$	1.41
$\bar{m}_b(\bar{m}_b)$/GeV	4.195(14)
$C_1^{(0)}$	−0.269
$C_2^{(0)}$	1.12
γ_0	0.505
γ_1	0.033
$\tilde{\gamma}_1$	−0.077
γ_2	−0.513
$\tilde{\gamma}_2$	−1.667
γ_3	0.026
$\tilde{\gamma}_3$	−0.060

Combining the leading term (17) with our result for the next-to-leading term (20) we find a Standard Model prediction for the $B_s^0 - \bar{B}_s^0$ width difference

$$\Delta\Gamma_s = 0.092(14)\ \text{ps}^{-1}\,. \tag{21}$$

The error in (21) is mostly due to the uncertainty in $\Delta\Gamma_{1/m_b}$; its variance contributes approximately 60% to the total variance in (21). The next largest uncertainty is due to the perturbative error in the first term of (17), which contributes a 30% proportion of the $\Delta\Gamma_s$ variance. The variance of B_1 contributes 8% of the total.

VII. CONCLUSIONS

Since, in the Standard Model, $\Delta\Gamma_s$ is dominantly due to processes with intrinsic charm, it is unlikely that new physics would contribute significantly to experimental measurements. Therefore, agreement between theory and experiment is an important test of the heavy quark expansion. The HFLAV average of experimental measurements prepared for PDG 2018 is $\Delta\Gamma_s = 0.088(6)$ ps^{-1} [39]. This is in good agreement with our result (21) with a much smaller uncertainty.

This work improves the Standard Model prediction for $\Delta\Gamma_s$ by using hadronic matrix elements computed using lattice QCD, removing reliance on the vacuum saturation approximation. In particular, matrix elements of the operators R_2 and R_3 (and $\tilde{R}_{2,3}$) have been computed for the first time. The resulting uncertainty in $\tilde{\Gamma}_{12,1/m_b}$ has been reduced compared to earlier, model-dependent estimates. More importantly, model dependence has been removed.

There remains more to do in order for the theoretical prediction to match the experimental precision. The next generation lattice calculation will require one-loop matching of lattice to $\overline{\text{MS}}$ regularization schemes in order to reduce the uncertainty in $\tilde{\Gamma}_{12,1/m_b}$. At the same time the work to determine the perturbative coefficients appearing in (17) through NNLO must be completed. First steps have already begun [13].

Acknowledgments: We thank the MILC collaboration for their gauge configurations and their code MILC-7.7.11 [40]. MW is grateful for an IPPP Associateship held while some of this work was undertaken and for discussions with A. Lenz. This work was funded in part by the STFC, the NSF, and the DOE. CJM is supported in part by the U.S. Department of Energy, Office of Science, Office of Nuclear Physics under contract Nos. DE-FG02-00ER41132 and DE-AC05-06OR23177. Results described here were obtained using the Darwin Supercomputer of the University of Cambridge High Performance Computing Service as part of the DiRAC facility jointly funded by STFC, the Large Facilities Capital Fund of BIS and the Universities of Cambridge and Glasgow.

[1] M. Beneke, G. Buchalla, and I. Dunietz, Phys. Rev. D **54**, 4419 (1996), arXiv:hep-ph/9605259, [Erratum: Phys. Rev. D **83**, 119902 (2011)].
[2] M. Artuso, G. Borissov, and A. Lenz, Rev. Mod. Phys. **88**, 045002 (2016), arXiv:1511.09466.
[3] N. Carrasco *et al.* (ETM Collaboration), J. High Energy Phys. **03**, 016 (2014), arXiv:1308.1851.
[4] Y. Aoki, T. Ishikawa, T. Izubuchi, C. Lehner, and A. Soni, Phys. Rev. D **91**, 114505 (2015), arXiv:1406.6192.
[5] A. Bazavov *et al.* (Fermilab Lattice, MILC Collaboration), Phys. Rev. D **93**, 113016 (2016), arXiv:1602.03560.
[6] R. J. Dowdall *et al.*, (2019), arXiv:1907.01025.
[7] S. Aoki *et al.* (Flavour Lattice Averaging Group Collaboration), (2019), arXiv:1902.08191.
[8] A. Lenz and U. Nierste, Numerical Updates of Lifetimes and Mixing Parameters of B Mesons, in *CKM unitarity triangle. Proceedings, 6th International Workshop, CKM 2010, Warwick, UK, September 6-10, 2010*, 2011, arXiv:1102.4274.
[9] E. Gamiz, J. Shigemitsu, and H. Trottier, Phys. Rev. D **77**, 114505 (2008), arXiv:0804.1557.
[10] C. Monahan, E. Gamiz, R. Horgan, and J. Shigemitsu, Phys. Rev. D **90**, 054015 (2014), arXiv:1407.4040.
[11] M. Beneke, G. Buchalla, C. Greub, A. Lenz, and U. Nierste, Phys. Lett. B **459**, 631 (1999), arXiv:hep-ph/9808385.
[12] A. Lenz and U. Nierste, J. High Energy Phys. **06**, 072 (2007), arXiv:hep-ph/0612167.
[13] H. M. Asatrian, A. Hovhannisyan, U. Nierste, and

A. Yeghiazaryan, J. High Energy Phys. **10**, 191 (2017), arXiv:1709.02160.
[14] A. Bazavov *et al.* (MILC Collaboration), Phys. Rev. D **82**, 074501 (2010), arXiv:1004.0342.
[15] A. Bazavov *et al.* (MILC Collaboration), Phys. Rev. D **87**, 054505 (2013), arXiv:1212.4768.
[16] A. Bazavov *et al.* (MILC Collaboration), Phys. Rev. D **93**, 094510 (2016), arXiv:1503.02769.
[17] E. Follana *et al.* (HPQCD Collaboration), Phys. Rev. D **75**, 054502 (2007), arXiv:hep-lat/0610092.
[18] A. Hart, G. M. von Hippel, and R. R. Horgan (HPQCD Collaboration), Phys. Rev. D **79**, 074008 (2009), arXiv:0812.0503.
[19] G. P. Lepage, L. Magnea, C. Nakhleh, U. Magnea, and K. Hornbostel, Phys. Rev. D **46**, 4052 (1992), hep-lat/9205007.
[20] R. J. Dowdall, C. T. H. Davies, R. R. Horgan, C. J. Monahan, and J. Shigemitsu, Phys. Rev. Lett. **110**, 222003 (2013), arXiv:1302.2644.
[21] G. P. Lepage *et al.*, Nucl. Phys. Proc. Suppl. **106**, 12 (2002), hep-lat/0110175.
[22] B. Colquhoun *et al.*, Phys. Rev. D **91**, 114509 (2015), arXiv:1503.05762.
[23] C. Davies *et al.*, EPJ Web Conf. **175**, 13023 (2018), arXiv:1712.09934.
[24] C. M. Bouchard, G. P. Lepage, C. Monahan, H. Na, and J. Shigemitsu, Phys. Rev. D **90**, 054506 (2014), arXiv:1406.2279.
[25] K. Hornbostel *et al.*, Phys. Rev. D **85**, 031504 (2012), arXiv:1111.1363.
[26] S. Collins *et al.*, Phys. Rev. D **63**, 034505 (2001).
[27] C. McNeile, C. T. H. Davies, E. Follana, K. Hornbostel, and G. P. Lepage, Phys. Rev. D **82**, 034512 (2010), arXiv:1004.4285.
[28] B. Chakraborty *et al.*, Phys. Rev. D **91**, 054508 (2015), arXiv:1408.4169.
[29] M. Wingate *et al.*, Phys. Rev. Lett. **92**, 162001 (2004).
[30] E. Dalgic *et al.*, Phys. Rev. D **76**, 011501 (2007), arXiv:hep-lat/0610104.
[31] R. J. Dowdall, C. T. H. Davies, G. P. Lepage, and C. McNeile, Phys. Rev. D **88**, 074504 (2013), arXiv:1303.1670.
[32] C. T. H. Davies, E. Follana, I. D. Kendall, G. P. Lepage, and C. McNeile (HPQCD Collaboration Collaboration), Phys. Rev. D **81**, 034506 (2010), arXiv:0910.1229.
[33] M. Tanabashi *et al.* (Particle Data Group Collaboration), Phys. Rev. D **98**, 030001 (2018).
[34] A. Bazavov *et al.*, Phys. Rev. D **98**, 074512 (2018), arXiv:1712.09262.
[35] M. Beneke, G. Buchalla, C. Greub, A. Lenz, and U. Nierste, Nucl. Phys. B **639**, 389 (2002), arXiv:hep-ph/0202106.
[36] A. T. Lytle, C. T. H. Davies, D. Hatton, G. P. Lepage, and C. Sturm (HPQCD Collaboration), Phys. Rev. D **98**, 014513 (2018), arXiv:1805.06225.
[37] N. Carrasco *et al.* (European Twisted Mass Collaboration), Nucl. Phys. B **887**, 19 (2014), arXiv:1403.4504.
[38] A. Bazavov *et al.* (Fermilab Lattice, MILC, TUMQCD Collaboration), Phys. Rev. D **98**, 054517 (2018), arXiv:1802.04248.
[39] Y. Amhis *et al.* (Heavy Flavor Averaging Group (HFAG) Collaboration), (2016), arXiv:1612.07233, and online update at https://hflav.web.cern.ch/.
[40] MILC Code Repository, https://github.com/milc-qcd.